



# Low-Frequency Dynamics and Its Correlation of Nanoscale Structures in Amorphous Solids

Weiming Yang<sup>1</sup> · Wenyu Li<sup>1</sup> · Qi Jiang<sup>2</sup> · Juntao Huo<sup>3</sup> · Yucheng Zhao<sup>1</sup> · Haishun Liu<sup>2</sup>

Received: 13 June 2019 / Accepted: 15 November 2019  
© Springer Science+Business Media, LLC, part of Springer Nature 2019

## Abstract

Unlike the crystalline solids, the atomic arrangements in amorphous solids lack long-range translational and orientational order. Despite intense research activity on their structures, the details of how the atoms are packed in amorphous solids remain mysterious at present. Here, we propose a structure feature like polymers and estimate the nanoscale of short-range order (SRO) and medium-range order (MRO) in this description according to the boson peak in amorphous solids. The result supports the concepts that (a) the low-frequency local vibrations are defined by the characteristic length of nanoscale clusters and (b) a decisive scale correlation of solvent atoms, SRO and MRO is about 1:3:7 in amorphous solids.

**Keywords** Amorphous solids · Nanoscale clusters · Short-range order · Medium-range order

---

**Electronic supplementary material** The online version of this article (<https://doi.org/10.1007/s10909-019-02268-6>) contains supplementary material, which is available to authorized users.

---

✉ Juntao Huo  
huojuntao@nimte.ac.cn

✉ Haishun Liu  
liuhaishun@cumt.edu.cn

<sup>1</sup> State Key Laboratory for Geomechanics and Deep Underground Engineering, School of Mechanics and Civil Engineering, China University of Mining and Technology, Xuzhou 221116, People's Republic of China

<sup>2</sup> School of Physical Science and Technology, China University of Mining and Technology, Xuzhou 221116, People's Republic of China

<sup>3</sup> Key Laboratory of Magnetic Materials and Devices, Ningbo Institute of Materials Technology and Engineering, Chinese Academy of Sciences, Ningbo 315201, People's Republic of China

## 1 Introduction

Peculiarities of amorphous structures on disordered atomic arrangement have been studied for more than 50 years [1–3]. The main question is what structure unit is in amorphous solids, like unit cell in crystalline materials. Because amorphous solids do not have any translational and rotational symmetry, it is quite difficult to experimentally characterize their atomic structure by X-ray or neutron diffraction, extended X-ray-absorption fine structure and nuclear magnetic resonance [4–7]. Various structural models, such as Bernal’s “dense random packing” [8], Gaskell’s “short-range order” [9] and the recent “solute-centered quasi-equivalent cluster” models [10, 11], have been proposed according to hypothesis or simulation in the past years. At present it has been accepted that a majority of the junctions among the short-range orders (SRO) and medium-range orders (MRO) are occupied by excess solvent atoms [12, 13]. However, it is still unclear whether a quantitative relation exists between correlation lengths of SRO and MRO in amorphous solids, and no clear picture relating the amorphous structure to the dynamical properties has been accepted [14]. These questions play the key role in characterizing the structure and reckoning the measurable physical properties from atomic structure in amorphous solids. From the dynamical point of view, low-frequency anomalies of vibration properties in amorphous solids as a result of quasilocal excitations, the so-called boson peak (BP), are frequently ascribed to structural correlations over an intermediate-range scale [15–17]. Although the nature of these quasilocal excitations is still under discussion [18], it has been supposed that they are connected with some correlation length of the amorphous structure [19, 20]. It may provide a possible method to understand the widespread feature of the amorphous structure.

In this paper, we have estimated the decisive scale of short- and medium-range atomic order, and their correlation according to the low-frequency (boson) peak in amorphous solids.

## 2 Experiments

Ten amorphous solids, with seven typical alloy systems including Fe-based, Co-based, Zr-based [21], PdCu-based [22], CuZr-based [23], Cu-based [24] and Pd-based metallic glasses [25], and three non-metallic glasses, were used in the present work (See Materials and Method in Supplemental Material for details). In the present study, metallic glasses of  $\text{Fe}_{64.8}\text{Co}_{7.2}\text{B}_{20}\text{Si}_4\text{Nb}_4$  and  $\text{Co}_{50.4}\text{Fe}_{21.6}\text{B}_{20}\text{Si}_4\text{Nb}_4$  were fabricated using copper-mold casting. Their glassy nature was ascertained by X-ray diffraction (D8 Advance) with Cu  $K\alpha$  radiation, a differential scanning calorimeter (NETZSCH DSC-404) with a heating rate of 40 K/min and transmission electron microscopy (Tecnai F20). The specific heat measurements were carried out between 3 and 53 K with specific heat option of the physical property measurement system from quantum design system (Model-9) with a disk shape

( $\sim 0.5$  mm thickness). According to the specifications, the relative error on the specific heat measurements on this instrument is less than 2%.

### 3 Results and Discussion

As examples, the phonon specific heat of three metallic glasses samples (See calculation method in Supplemental Material for details) is shown in Fig. 1. Being different from phonon specific heat of crystalline materials, that of metallic glasses may not be described by the Debye model only [26]. It has been known that localized harmonic vibration modes may exist in amorphous materials [27]. These localized vibrations result in additional Einstein-type vibration, i.e., localized harmonic vibration with a specific frequency [28, 29]. However, if we assume that the phonon specific heat of the MGs results from the Debye-type and only one Einstein-type vibration modes, the phonon specific heat still deviates somewhat from the model [23, 30]. Fortunately, we find that the addition of two quantized harmonic Einstein-type vibration modes are required in order to model the phonon specific heat of metallic glasses. Figure 1 shows the fitting of measured phonon specific heat using models including the contribution of two Einstein oscillators. The red lines through the Boson peak data in Fig. 1 represent a fit to the equation:

$$C_{\text{Phonon}} = aC_{D(A)} + bC_{E(B)} + cC_{E(C)} \quad (1)$$

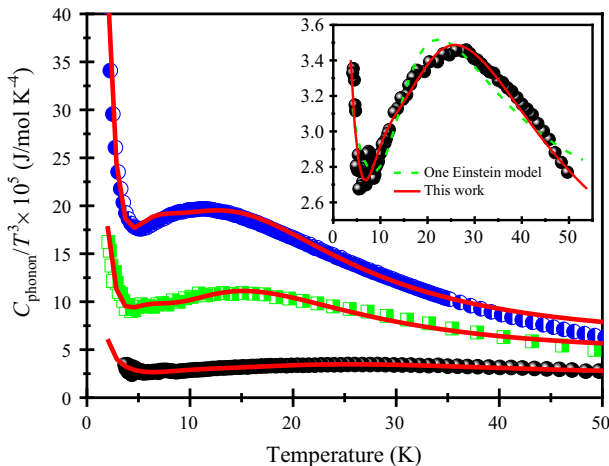


**Fig. 1** Photonic specific heat divided by cube of temperature versus temperature for  $\text{Pd}_{41.25}\text{Cu}_{41.25}\text{P}_{17.5}$ ,  $\text{Zr}_{46.75}\text{Ti}_{8.25}\text{Cu}_{7.5}\text{Ni}_{10}\text{Be}_{27.5}$  and  $\text{Fe}_{64.8}\text{Co}_{7.2}\text{B}_{20}\text{Si}_4\text{Nb}_4$  metallic glasses from top to down, respectively. The red lines through the data are based on a calculation that the contribution from two Einstein oscillators is added to the Debye oscillators. Inset: Zoom-in of the  $\text{Fe}_{64.8}\text{Co}_{7.2}\text{B}_{20}\text{Si}_4\text{Nb}_4$  data. The green dashed line through the data is based on a hypothesis that one kind of Einstein oscillators exist besides Debye oscillators (Color figure online)

Here,  $a$ ,  $b$  and  $c$  are the weight factors for the three types of oscillators that represent contributions from Debye-type and Einstein-type oscillators.  $C_D = 12\pi^4 Rk_B^3 T^3 / 5(\hbar\omega_A)^3$  is the Debye function, with Debye-type vibrational frequency  $\omega_A$ .  $C_{E(i)} = 3R(\hbar\omega_i/k_B T)^2 e^{\hbar\omega_i/k_B T} / (e^{\hbar\omega_i/k_B T} - 1)^2$  ( $i=B$  and  $C$ ) is the Einstein function, with two Einstein-type vibrational frequencies  $\omega_B$  and  $\omega_C$ , respectively. The fact that two Einstein oscillators are required to model the data indicates that two distinct local modes may exist in the glasses, which is in excellent agreement with the density of vibrational states obtained from the neutron scattering measurements [31, 32].

Figure 2 shows the comparisons of  $\omega_A$ ,  $\omega_B$  and  $\omega_C$  for seven kinds of metallic glasses from the above calculation and Debye frequency of their pure base metal polycrystalline in the literature [33], respectively. From comparisons of the calculation and experimental results of the Debye frequency  $\omega_A$  for the BMG systems, the calculation results are consistent with experimental results [34]. Moreover, the relationship between vibration frequency and radius of solvent components [35] are also compared. The parameters,  $\omega_A$ ,  $\omega_B$  and  $\omega_C$  as well as  $a$ ,  $b$  and  $c$ , are summarized in Table S1. It is striking to see that Debye frequencies of most metallic glasses are very close to those of the base metal. For instance, the Debye frequency of  $Zr_{46.75}Ti_{8.25}Cu_{7.5}Ni_{10}Be_{27.5}$  is  $3.902 \times 10^{13}/s$  in the present work, almost identical to that of pure polycrystalline Zr ( $3.809 \times 10^{13}/s$ ) [33], whereas this value is much smaller than those of other components, i.e.,  $5.498 \times 10^{13}/s$  of Ti, ( $4.490 \times 10^{13}/s$ ) Cu, ( $5.891 \times 10^{13}/s$ ) Ni and ( $18.850 \times 10^{13}/s$ ) Be. For some bimetal-based glassy systems such as  $Pd_{41.25}Cu_{41.25}P_{17.5}$  and  $Cu_{50}Zr_{50}$ , the Debye frequencies are not close to those of their component Cu, but close to those of Pd and Zr which are their solvent elements, respectively [13]. We also found that a general rule that  $\omega_C < \omega_B < \omega_A$  for different compositions and the vibrational frequency tends to be inversely proportional to radius of the solvent component in metallic glasses. They indicate the vibrations of metallic glasses likely inherited from the solvent components. In fact, not only the Debye frequency but also the elastic modulus and electronic structure

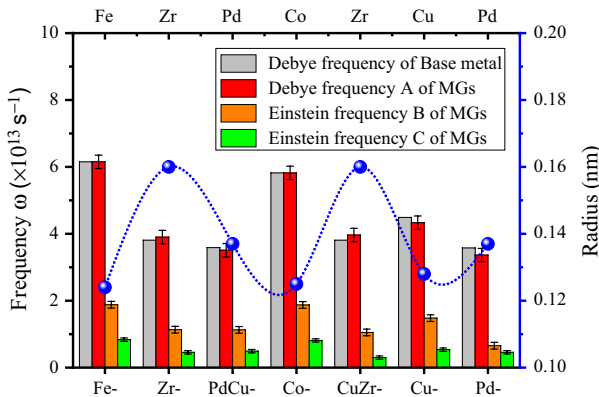


**Fig. 2** Histograms of vibrational frequency for seven kinds of metallic glasses and their solvent elements. Also shown are the radii of solvent elements (Color figure online)

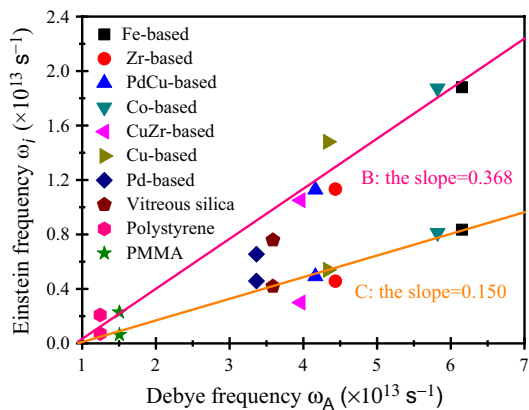
in amorphous solids can inherit from their solvent components [12, 13, 36, 37]. The structural features of amorphous solids can be understood by the analogy with polymers as they are both formed by a hierarchy of bonding forces [12]. The polymers are basically molecules linked by van der Waals forces, while the amorphous solids can be viewed as the strongly bonded solute-centered solute–solvent clusters linked by relatively weak solvent–solvent bonds. For instance, bonds of Zr–Cu, Zr–Ni and Zr–Al in Vit105 are much stronger than Zr–Zr, as indicated by their large negative values of enthalpy of mixing [38], which are  $-23$ ,  $-49$  and  $-44$  kJ/mol, respectively. In this regard, the atoms in clusters or superclusters vibrate together. In harmonic vibrational analysis, the vibrational frequencies  $\omega_i$  of these normal modes are given by

$$\omega_i = 2\pi\sqrt{\frac{\alpha}{M_i}}, \quad (i = A, B \text{ and } C) \quad (2)$$

where  $\alpha$  is the bonding force constant,  $M_i$  is the mass of oscillator,  $A$ ,  $B$  and  $C$  are the same as in Eq. (1). From this point of view, it is reasonable to conclude that the bonds linking the oscillators are almost equal to and primarily determined by its solvent–solvent bonds, and then we have  $M_C > M_B > M_A$ . It can safely be said that the solute-centered clusters ( $B$ ) and the superclusters ( $C$ ) will behave like a quasi-continuum region, resulting in localized modes that are responsible for the BP in glasses. A majority of the junctions among  $B$  and  $C$  are also occupied by excess solvent atoms ( $A$ ) in the amorphous materials. This interpretation hence supports the cluster modes as the microscopic origin of the BP. That is, amorphous solids can be regarded as a collection of the clusters yielding the transverse-type acoustic modes localized on the short- and medium-range length scale, and this localized dynamic is most probably responsible for the anomalous low-frequency behavior of glasses, or the BP.

Upon analyzing the Einstein and Debye frequency data of various amorphous solids, we found that indeed strong linear relations exist between the Einstein and Debye frequency, as shown in Fig. 3. It is interesting to note that the slope of lines

**Fig. 3** Relationship among Einstein and Debye frequency for ten kinds of amorphous solids cover five typical alloy systems and three non-metallic glasses. The solid lines represent linear fits to the data (Color figure online)



is about 0.368 and 0.150 among glasses of completely different chemical compositions. It indicates that  $\omega_A \approx 3\omega_B \approx 7\omega_C$  is an intrinsic property of amorphous solids [17]. In a harmonic vibrational analysis, the acoustic mode in an elastic continuum exhibits the proportionality of frequency to wave number  $q_i$ . For a linear chain with the same spacing  $a$  and the same force constant  $\alpha$ , the frequency of the acoustic mode  $\omega_i/2\pi$  can be written as

$$\omega_i \approx 2\sqrt{\frac{\alpha}{M_i}} \left| \sin\left(\frac{1}{2}aq_i\right) \right| \quad (3)$$

If the acoustic mode concept is applicable to the present low-frequency vibrational modes, we have  $\omega_i \propto q_i$  for  $q_i$  near 0. This relationship allows one to assume that the vibrational frequency of the nanoscale cluster in the BP region is determined by the “wave number” or “wave length” of the vibrational modes that match the boundary condition of the respective atomic oscillators.

Another point of view of this phonon localization behavior is in terms of the Ioffe-Regel condition [19], where the limiting value of the mean-free path  $l$  in the strong-scattering limit, corresponding to the onset of localization, is given by

$$q \approx \frac{2\pi}{l} \quad (4)$$

where  $q$  is the wave number. The minimum value for the mean-free path,  $l$ , is determined by the size of the particles causing the scattering [39] or, in the present case, by the nanoscale of oscillators in amorphous solids. Indeed, as mentioned previously, the “wave number” of the present vibrational modes appears to become longer with increasing  $\omega$ , and the fundamental vibrational frequency of the localization modes increases with decreasing localization length or correlation length of oscillators. Then  $\omega_i \propto 1/r_i$ , this explains why the vibrational frequency tends to be inversely proportional to the radius of the solvent element in metallic glasses. Meanwhile, it indicates that  $r_A:r_B:r_C \approx 1:3:7$ , where  $r_A$ ,  $r_B$  and  $r_C$  are the outer radius of structural units  $A$ ,  $B$  and  $C$ , respectively. In the following, we describe a physical model to illustrate this correlation in detail.

The local atomic structure in amorphous solids can be illustrated in Fig. 4, the solute-centered clusters ( $B$ ) are characterized by SRO, each of which is made up of a solute atom surrounded by a majority of solvent atoms ( $A$ ) [12]. The superclusters ( $C$ ) are characterized by MRO, each of which is constructed by packing of the clusters beyond the SRO. Here, if we assume that the radius of solvent and solute atoms are not very different, the outer diameters of the SRO and MRO are approximately 3 and 7 times the diameter of the atoms of the solvent element in amorphous solids, respectively. This explains why the Einstein frequency tends to be proportional to the Debye frequency in glasses. For instance, the radius of Zr in  $\text{Zr}_{66.7}\text{Ni}_{33.3}$  metallic glass is 0.16 nm [35], as indicated the outer diameter of SRO and MRO is about 0.96 and 2.24 nm, respectively. The result is in excellent agreement with the local atomic order obtained from the direct observation [40] and ab initio molecular dynamics simulations [10, 11].

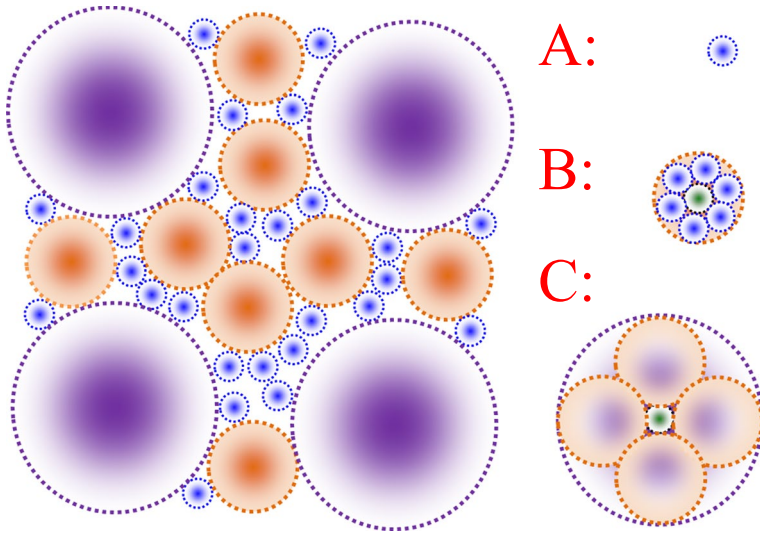


**Fig. 4** Schematic illustration of a hypothetical amorphous structure showing local packing of solvent atoms (A), SRO (B) and MRO (C) in the amorphous solid. The B and C denote the outmost atomic shell filled with a majority of solvent atoms. Each of B is made up of a solute atom surrounded by a majority of A. Each of C represents the inner solute atoms surrounded by majority of clusters beyond the SRO. The correlations radius of B and C is about 3 and 7 times of that of A, respectively (Color figure online)

From the analysis of our results as well as literature data, we can also conclude tentatively that the correlation radius of the atomic order region in the metallic glassy structure is formed in the supercooled melt. The correlation length is essentially a thermodynamic equilibrium property, which is, however, strongly dependent on the radius of solvent elements in the glasses. Liu et al. revealed that the atomic packing in amorphous alloys can be described globally by the spherical-periodic orders [41]. For the shell number  $i > 6$ , it has been verified  $g(r_i) \rightarrow 1$  correspondingly for most amorphous alloys [42]. Because the atomic radius of most metal solvent elements is about 0.124–0.183 nm [35], the decisive scale of SRO and MRO in metallic glasses is about 0.74–1.1 nm and 1.7–2.6 nm, respectively. Then, the scales of MRO and SRO in amorphous solids are approximately 7 and 3 times the average diameter of the atoms, respectively, which agrees with the HRTEM results [17]. Recently, a strong correlation was also revealed between vibration frequencies and the local atomic packing [43]. This happens in many cases that changing the chemical elements without significant variation of the structural units, but rather only with a change of correlation in their arrangement. The deviation (see Fig. 3) can be attributed by the radius of added elements which are often larger or smaller than the radius of solvent atoms. In the case of covalent amorphous materials ( $\text{SiO}_2$ ), where directed bonding is dominant, SRO can be characterized by different types of atoms constituting the coordination polyhedron centered on a particular atom (Si) [44]. The definition of MRO is more contentious, but it can simply be regarded as the 2nd highest level of structural organization beyond SRO. Since the local atomic order in covalent amorphous materials (3.3 nm for  $\text{SiO}_2$  and 4.2 nm for PMMA) [39] is

larger than in most metallic glasses, the correlation between SRO and MRO still exists in this kind of amorphous systems.

The atomic interactions within SRO and MRO are stronger, while the solvent–solvent interactions linking the SRO and MRO are much weaker. The elastic deformation in amorphous solids mainly occurs at the solvent–solvent junctions among solute-centered clusters and/or superclusters, and that the moduli are essentially determined by the weakest solvent–solvent bonding [36]. Thus, the atomic interactions heterogeneities are important for the elastic heterogeneities in amorphous solids. On the one hand, the SRO length-sized clusters and MRO length-sized superclusters in amorphous alloys could vibrate like quasi-continuum regions and result in the localized harmonic modes for the BP peak. On the other hand, the amorphous solids exhibit spatially inhomogeneous elastic moduli, with coexistence of hard and soft regions on the scale of a few tens of particles. The position and amplitude of the BP were controlled by the elastic modulus value and heterogeneity [45, 46].

Recent studies also have revealed that the localized vibrations follow the non-Debye scaling law: the density of states  $D(\omega) \propto \omega^4$  [47], which is different from the Debye law  $D(\omega) \propto \omega^2$ . If the effects of phonons are suppressed by introducing a random potential [48], tuning the system size to be sufficiently small [47], focusing on the low-frequency regime below the lowest phonon mode [49], or dividing into soft localized mode [50], the  $\omega^4$  law can be observed in the amorphous solids. In the present work, we found that the vibrational modes can be divided into a Debye phonon mode and two Einstein modes. Obviously, there is some sort of association between these different modes, but these associations require further study.

## 4 Conclusion

In summary, we have for the first time demonstrated a close correlation between the radiuses of solvent elements, SRO and MRO according to the low-frequency anomalies of vibration properties in amorphous solids. Our work offers quantitative relations between correlation lengths of SRO and MRO. The finding is critical for understanding not only the nature of BP, but also the characterization of local atomic order, which may provide an approach to characterize the local atomic order and reckon the measurable physical properties from atomic structure in amorphous solids.

**Acknowledgements** The authors would thank the reviewers for their valuable comments and suggestions on this paper. This work was supported by the National Natural Science Foundation of China (Nos. 51871237, 51631003 and 51771217), and Xuzhou Key Research & Development Program (KC17015). We thank V. A. Khonik of State Pedagogical University, W. H. Wang and M. B. Tang of Chinese Academy of Sciences for providing the specific heat data of  $\text{Pd}_{41.25}\text{Cu}_{41.25}\text{P}_{17.5}$ ,  $\text{Cu}_{50}\text{Zr}_{50}$  and  $\text{Zr}_{46.75}\text{Ti}_{8.25}\text{Cu}_{7.5}\text{Ni}_{10}\text{Be}_{27.5}$  metallic glasses, respectively.

## References

1. P. Duwez et al., *J. Appl. Phys.* **31**, 1136 (1960)
2. W.L. Johnson, *Prog. Mater. Sci.* **30**, 81 (1986)
3. A. Inoue et al., *Nat. Mater.* **2**, 661 (2003)
4. Y.Q. Cheng, E. Ma, H.W. Sheng, *Phys. Rev. Lett.* **102**, 245501 (2009)
5. D. Ma, A.D. Stoica, X.-L. Wang, *Nat. Mater.* **8**, 30 (2009)
6. T. Fujita et al., *Phys. Rev. Lett.* **103**, 075502 (2009)
7. K.X. Xi et al., *Phys. Rev. Lett.* **99**, 095501 (2007)
8. J.D. Berbal, *Nature* **185**, 68 (1960)
9. P.H. Gaskell, *Nature* **276**, 484 (1978)
10. D.B. Miracle, *Nat. Mater.* **3**, 697 (2004)
11. H.W. Sheng et al., *Nature* **439**, 419 (2006)
12. D. Ma et al., *Phys. Rev. Lett.* **108**, 085501 (2012)
13. W.H. Wang, *J. Appl. Phys.* **111**, 123519 (2012)
14. B. Ruta et al., *Phys. Rev. Lett.* **109**, 165701 (2012)
15. T. Uchino, T. Yoko, *J. Chem. Phys.* **108**, 8130 (1998)
16. V.K. Malinovsky et al., *Europhys. Lett.* **11**, 43 (1990)
17. W.M. Yang et al., *J. App. Phys.* **116**, 123512 (2014)
18. N. Jakse, A. Nassour, A. Pasturel, *Phys. Rev. B* **85**, 174201 (2012)
19. S.R. Elliott, *Europhys. Lett.* **19**, 201 (1992)
20. A.P. Sokolov et al., *Phys. Rev. Lett.* **69**, 1540 (1992)
21. M.B. Tang et al., *Appl. Phys. Lett.* **86**, 021910 (2005)
22. A.N. Vasiliev et al., *Phys. Rev. B* **80**, 172102 (2009)
23. M.B. Tang, H.Y. Bai, W.H. Wang, *Phys. Rev. B* **72**, 012202 (2005)
24. Z.X. Wang, B. Sun, J.B. Lu, *Trans. Nonferrous Met. Soc. China* **21**, 1309 (2011)
25. H.S. Chen, W.H. Haemmerle, *J. Non-Cryst. Solids* **11**, 161 (1972)
26. A.P. Sokolov et al., *Phys. Rev. Lett.* **78**, 2405 (1997)
27. A.V. Granato, *Phys. B* **219–220**, 270 (1996)
28. Z.H. Zhou et al., *Appl. Phys. Lett.* **89**, 031924 (2006)
29. Y. Li et al., *J. Appl. Phys.* **104**, 013520 (2008)
30. Y. Li et al., *Phys. Rev. B* **74**, 052201 (2006)
31. A. Meyer et al., *Phys. Rev. B* **53**, 12107 (1996)
32. V. Keppens et al., *Nature* **395**, 876 (1998)
33. C. Kittel, *Introduction to Solid State Physics*, 8th edn. (Beijing, Beijing, 2005), p. 86. **Chinese Ed.**
34. B. Golding, B.G. Bagley, F.S.L. Hsu, *Phys. Rev. Lett.* **29**, 68 (1972)
35. J.G. Speight, *Lang's Handbook of Chemistry*, 16th edn. (Mc Graw-Hill, London, 2005), p. 1.151
36. W.H. Wang, *Nat. Mater.* **11**, 275 (2012)
37. G. Li et al., *Phys. Rev. Lett.* **109**, 125501 (2012)
38. A. Takeuchi, A. Inoue, *Mater. Trans.* **46**, 2817 (2005)
39. J.E. Graebner, B. Golding, L.C. Allen, *Phys. Rev. B* **34**, 5696 (1986)
40. A. Hirata et al., *Nat. Mater.* **10**, 28 (2011)
41. X.J. Liu et al., *Phys. Rev. Lett.* **105**, 155501 (2010)
42. Y. Suzuki, J. Haimovich, T. Egami, *Phys. Rev. B* **35**, 2162 (1987)
43. A.S. Ahmad et al., *J. Low Temp. Phys.* **186**, 172 (2017)
44. S.R. Elliott, *Nature* **354**, 445 (1991)
45. F. Leonforte et al., *Phys. Rev. B* **72**, 224206 (2005)
46. H. Mizuno, S. Mossa, J.-L. Barrat, *Europhys. Lett.* **104**, 56001 (2013)
47. E. Lerner, G. During, E. Bouchbinder, *Phys. Rev. Lett.* **117**, 035501 (2016)
48. M. Baity-Jesi et al., *Phys. Rev. Lett.* **115**, 267205 (2015)
49. E. Lerner, G. During, *SciPost. Phys.* **1**, 016 (2016)
50. H. Mizuno, H. Shiba, A. Ikeda, *Proc. Natl. Acad. Sci. U.S.A.* **114**, E9767 (2017)